

# ISTITUTO NAZIONALE DI FISICA NUCLEARE

Sezione di Genova

---

INFN/AE-~~88~~<sup>87</sup>  
16 Ottobre 198~~8~~<sup>87</sup>

F. Fontanelli, P. Ramella and S. Vitale:

**CHARGE COLLECTION IN PARTIALLY DEPLETED SILICON DETECTORS**

## Charge collection in partially depleted silicon detectors

F.Fontanelli, P.Ramella, S.Vitale

I.N.F.N. Sezione di Genova and  
Dipartimento di Fisica—Università di Genova

### Abstract

The behaviour of partially depleted silicon detectors deserves some attention in the design of large systems as electromagnetic or hadronic calorimeters in which these detectors are used and conservative operating conditions must be imposed (1,2,3).

We have experimentally investigated charge collection from the undepleted region in silicon detectors manufactured for high energy calorimetry by Ansaldo Semiconductors S.p.A.

The observed results are compared with a simple model.

### Introduction and experimental method.

The detectors are ion implanted planar  $p^+n^-n^+$  diodes. The starting material is a 6 k $\Omega$  cm n-type silicon wafer, 400  $\mu$ m thick.

On a single wafer one large area detector (28 cm<sup>2</sup>) and 14 small detectors (1 cm<sup>2</sup>) with different edge design were produced. We have examined the behaviour of big detectors and of small ones with similar edge geometry. As no significant difference was found, apart the noise level, in the detailed investigation reported here, only the 1 cm<sup>2</sup> units were used.

The depletion depth, starting at the top  $p^+n$  junction, for each value of the applied inverse bias voltage  $V_b$ , and the voltage  $V_d$  for complete depletion, are determined from the V-C characteristics of the device. (fig. 1) The behaviour of the detector was investigated with electrons crossing the detector and with  $\alpha$  particles.

a) Electrons. When the integration time is 1  $\mu$ sec. or more, the pulse height distribution due to ionizing particles crossing the detector, whose maximum for applied bias voltage lower than  $V_d$ , decreases slower than the depletion depth, shows an indication of charge contribution from the undepleted region.

More detailed information can be achieved by analyzing the pulse shape. The transient averaging technique is essential to extract the relevant pulse features from noise.

The experimental set-up was realized as follows: the detector and a charge sensitive preamplifier with well known and simple pulse response were connected to a digital scope and the average pulse shape over 256 transients was recorded; the scope was triggered by conversion electrons from a  $\text{Cs}^{137}$  source that, after crossing the detector under test, reached a second silicon counter. For a fully depleted detector, ( $V_b > V_d$ ), charge collection is completed in a time short with respect to the sampling period and the shape of the output pulse coincides with the pulse response to a deltalike current input; pulse amplitude and shape are unaffected by increasing  $V_b$ . When  $V_b < V_d$ , after the fast rise, that decreases in amplitude as  $\sqrt{V_b/V_d}$ , a slowly rising contribution appears, that can be attributed to charge collection from the undepleted region. As easily shown by Z transform technique, due to our simple response function, the current and the integrated charge are almost exactly computed from the sampled voltages  $V(i)$  at the preamplifier output by the formulas:

$$I(i) = \frac{C}{T}(V(i-1)\beta T - V(i))$$

and

$$Q(i) = C(\beta T \sum V(i) - \sum V(i))$$

where  $T$  is the sampling period and  $\beta$  is the decay constant of the unit pulse response.

The main results of this analysis are:

- 1) The charge contribution due to the fast component of the current is proportional to  $\sqrt{(V_b/V_d)}$ , that is to the depletion depth. See fig. 3.
- 2) The risetime of the slow component decreases with  $V_b$ .
- 3) Increasing the integration time, the collected charge approaches an asymptotic value nearly independent on  $V_b$  and roughly equal to the charge collected when the detector is fully depleted.

A quantitative analysis of the time behaviour of the slow component is difficult, as in this condition the pulse current is of the order of .1 nAmp or less and it is superimposed to the steady inverse current of the diode, orders of magnitude higher.

b)  $\alpha$  particles.

A clearer comparison of the processes involved in charge collection from the depleted and from the neutral region, in less severe noise to signal conditions, is obtained by irradiating the "top"  $p^+n$  or the "back"  $n^-n^+$  junction with 5.4 Mev  $\alpha$  particles from an  $\text{Am}^{241}$  source.

Indeed, as the  $\alpha$  particles range in silicon is about 30  $\mu m$ , and dead layers are negligible on both the top  $p^+n$  and the back  $nn^+$  junction, in the first case only the depletion region and in the second only the neutral one are interested. The averaged pulse shape recorded in the two conditions for  $V_b = 120., 90., 60., 30., 15.$  volts corresponding to undepleted depths of 16, 67, 128, 208, 264  $\mu m$ , are shown in fig. 4. We note that at 120. volts the  $\alpha$  particles range exceeds the undepleted thickness.

The digital scope was operated at 20  $\mu sec./div$ , corresponding to a sampling period  $\Delta T = 400$  nsec. Internal trigger was used.

### Results and discussion.

The main results obtained by digital deconvolution are summarized in table I.

In the top condition the pulse current is shorter than the sampling period, as expected; the collected charge  $Q_0$  is independent from  $V_b$  within 1 % for  $V_b$  ranging from 30 to 120 volts, a decrease of 3% is observed at 15 volts. For  $V_b = 3$  volts the loss is 14 %.

In the "back" condition the current pulse is slow; the risetime  $\Delta T$  of the integrated charge (from 10 % to 90 % of the asymptothyc value  $Q$  of the collected charge in this condition) increases from 1.6 to 43  $\mu\text{sec}$  as  $V_b$  is decreased from 120 to 15 volts, but  $Q/Q_0$  is approaching nearly unity also for low  $V_b$ . The dependence of  $Q/Q_0$  vs the undepleted depth is shown in fig.5.

In fig 4 the integrated charge and the current vs time are reported. Dashed lines are computed assuming that the charge carriers produced in the neutral region migrate to the depletion region under the combined effect of diffusion and drift in an effective (uniform ) electric field  $E(V_b)$ .

Values of holes diffusion coefficient  $D$  and mobility  $\mu$  are taken from ref (5).

In order to fit the  $Q/Q_0$  dependence on the thickness of the undepleted region, the diffusion lenght of the charge carriers is assumed to be  $L_d = 2.4 \text{ mm}$ .

The parameter  $E$  is easily determined requiring the agreement between observed and computed rise time  $\Delta T$  of the  $Q/Q_0$  signal; the dependence of  $\Delta T$  on  $E$  is indeed very critical resulting in an the estimated error for  $E$  below 10 %. Vanishing values of  $E$  are incompatible with observed risetimes. The resulting values, reported in table I, roughly follow the empirical relation :

$$E(V_b) = (.8 + .05 V_b) \quad (\text{Volt/cm})$$

According to our definition of  $E(V_b)$ , this parameter can be related, in first approximation, to the real field  $E^*(x)$ , acting in the undepleted region through the relation:

$$\frac{1}{E(V_b)} = \frac{1}{\delta} \int_0^\delta \frac{dx}{E^*(x)}$$

$\delta$  being the thickness of the undepleted depth.

This relation is very natural, as  $\Delta T$  is inversely proportional to the drift velocity and hence to  $E^*$  when diffusion is negligible.

From  $E(V_b)$  we compute the average charge carriers density  $\langle p \rangle$  in the undepleted region, using the relation:

$$J = e\mu p E - eD \frac{dp}{dx}$$

were  $p$  is the local hole density; we take

$$\frac{1}{p} \frac{dp}{dx} = \frac{1}{L_d}$$

According to the usual short diode approximation(4), we assume a linear dependence of  $p$  on the distance from the depletion region, with a slope determined by the diffusion lenght  $L_d$ .

It results :

$$\langle p \rangle = p(0) + \frac{p^0 \delta}{L_d 2}$$

were  $p(0)$  is the hole density at the edge of the depletion region.

Values of  $\langle p \rangle$  are reported in the last column of table I.

From the slope in the plot of  $\langle p \rangle$  vs.  $\delta$  (fig. 6), we find the equilibrium hole density

in our material  $p^0 \approx 6 \cdot 10^8$ , in very reasonable agreement with what expected on the basis of material resistivity.

Hole density near the depletion region  $p(0)$  results about  $3 \cdot 10^7 \text{ cm}^{-3}$ .

**Conclusions:** Our measurements put in evidence the effect of the residual electric field on charge collection from the neutral (undepleted) region of silicon detectors; dealing with such phenomena, the field free approximation for the neutral region is clearly inadequate.

This residual field, that is  $\approx 3$  orders of magnitude smaller than in the depleted region, allows an almost 100 % efficient charge collection from the full thickness of the detector if the signal integration time is long enough and the material quality grants a value of  $L_d > \delta$ .

Charge collection times and efficiencies could be empirically determined with an  $\alpha$  particles source irradiating the "bottom" side of the detector by the simple method outlined here.

Evaluation by a model could be also made, but reliable values of material resistivity and hole diffusion length are needed; the high value of hole density at the brink of the depletion region that we have observed, suggest that a self consistent treatment of charge carriers and field distributions, should be considered.

#### REFERENCES

- 1) P. G. Rancoita, J.Phys. G10 (1984) 299
- 2) G. Barbiellini, G.Cecchet, J.Y.Hemery, F.Lemeilleur, C.Leroy, G.Levman, P.G.Rancoita and A.Seidman Nucl. Instr. and Meth. A236 316.
- 3) G.Barbiellini, P.Buksh, G.Cecchet, J.Y.Hemery, F.Lemeilleur, C.Leroy, G.Levman, P.G. Rancoita and A.Seidman, Nucl. Instr. and Meth. A235 55.
- 4) See e.g. A. Van der Zeil: Solid state physical electronics. Prentice Hall 1968.
- 5) E.E. Haller IEEE Transactions on Nuclear Science, Vol NS 29,V<sup>0</sup> 3, 1982 pg. 1109

Table 1

Vb	J (nA)	$\delta(\mu m)$	$Q/Q_{0\text{exp}}$	$Q/Q_{0c}$	$\Delta T(\mu sec)$	E (V/cm)	$\langle p \rangle$
120	29	16	.98	.99	1.6	6.9	$3.3 \cdot 10^7$
90	26.5	67	.95	.97	5.6	5.3	$4.0 \cdot 10^7$
60	22.3	128	.93	.95	14.	3.7	$4.8 \cdot 10^7$
30	16.5	208	.90	.90	30.4	2.4	$5.6 \cdot 10^7$
15	12.5	264	.84	.81	44.8	1.6	$6.5 \cdot 10^7$

## Figure Captions

Fig 1. Current and Capacitance vs. Inverse Bias Voltage for a typical  $1 \text{ cm}^2$  detector.

Fig 2. Typical averaged pulse obtained from the  $\beta$  source for different bias voltage before digital deconvolution.

Fig 3. Fast pulse component for conversion electrons, that is pulse height after  $0.5 \mu s$  from trigger

Fig 4. Average preamplifier output for  $\alpha$  particles before digital deconvolution.  
a) top side. b) bottom side

Fig 5. Collected charge pulse for  $\alpha$  particles (bottom side) obtained by digital deconvolution. Results of our model are shown as dashed lines.

Fig 6.  $Q/Q_0$  vs.  $\delta$  (undepleted depth).

Q is the total charge delivered by  $\alpha$  particles impinging on the bottom side and  $Q_0$  on the top side.

Fig 7.  $\langle p \rangle$  (local hole density) vs  $\delta$  (undepleted depth).

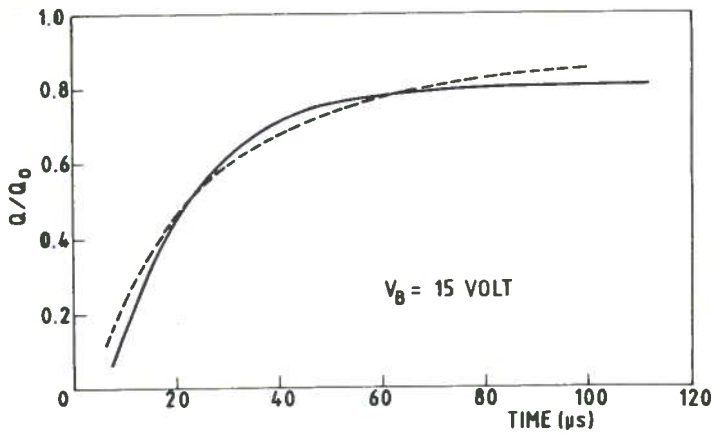


FIG 5-1

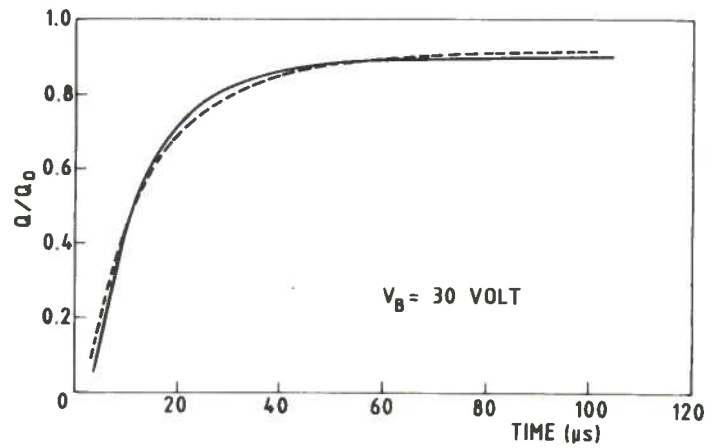


FIG 5-2

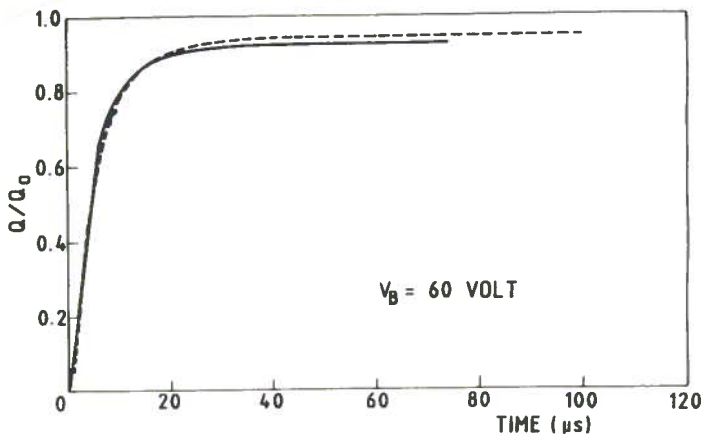


FIG 5-3

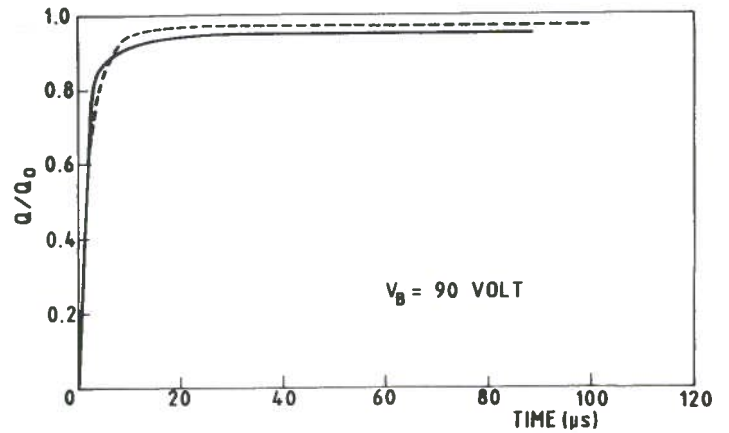


FIG 5-4

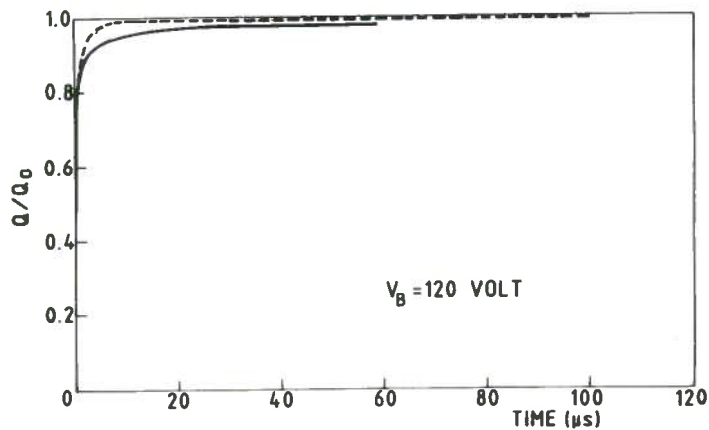


FIG 5-5

Fig 5. Collected charge pulse for  $\alpha$  particles (bottom side) obtained by digital deconvolution. Results of our model are shown as dashed lines.

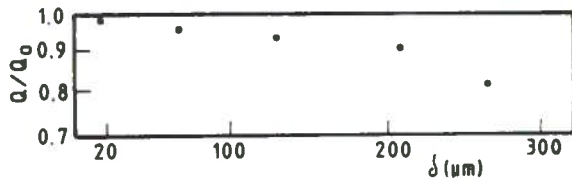


Fig 6.  $Q/Q_0$  vs.  $\delta$  (undepleted depth).  
 $Q$  is the total charge delivered by  $\alpha$  particles impinging on the bottom side and  $Q_0$  on the top side.

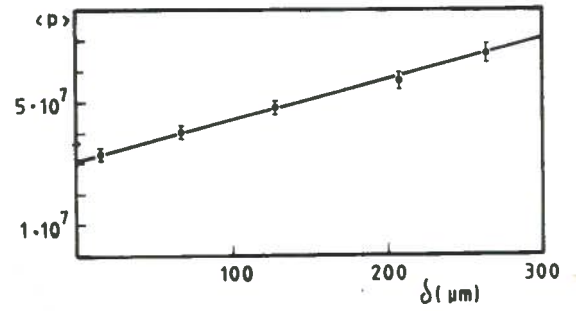


Fig 7.  $\langle p \rangle$  (local hole density) vs  $\delta$  (undepleted depth).



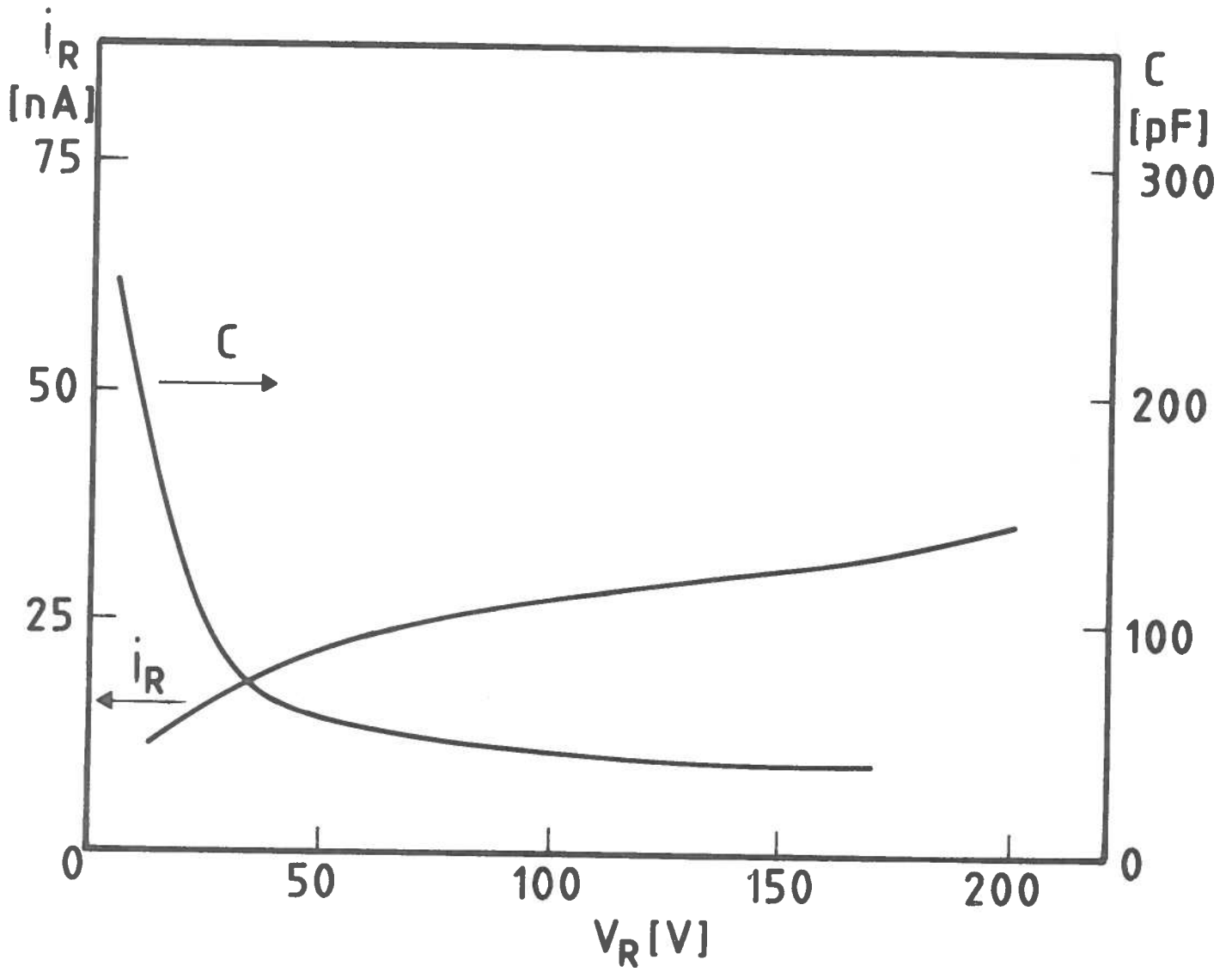


FIG.1

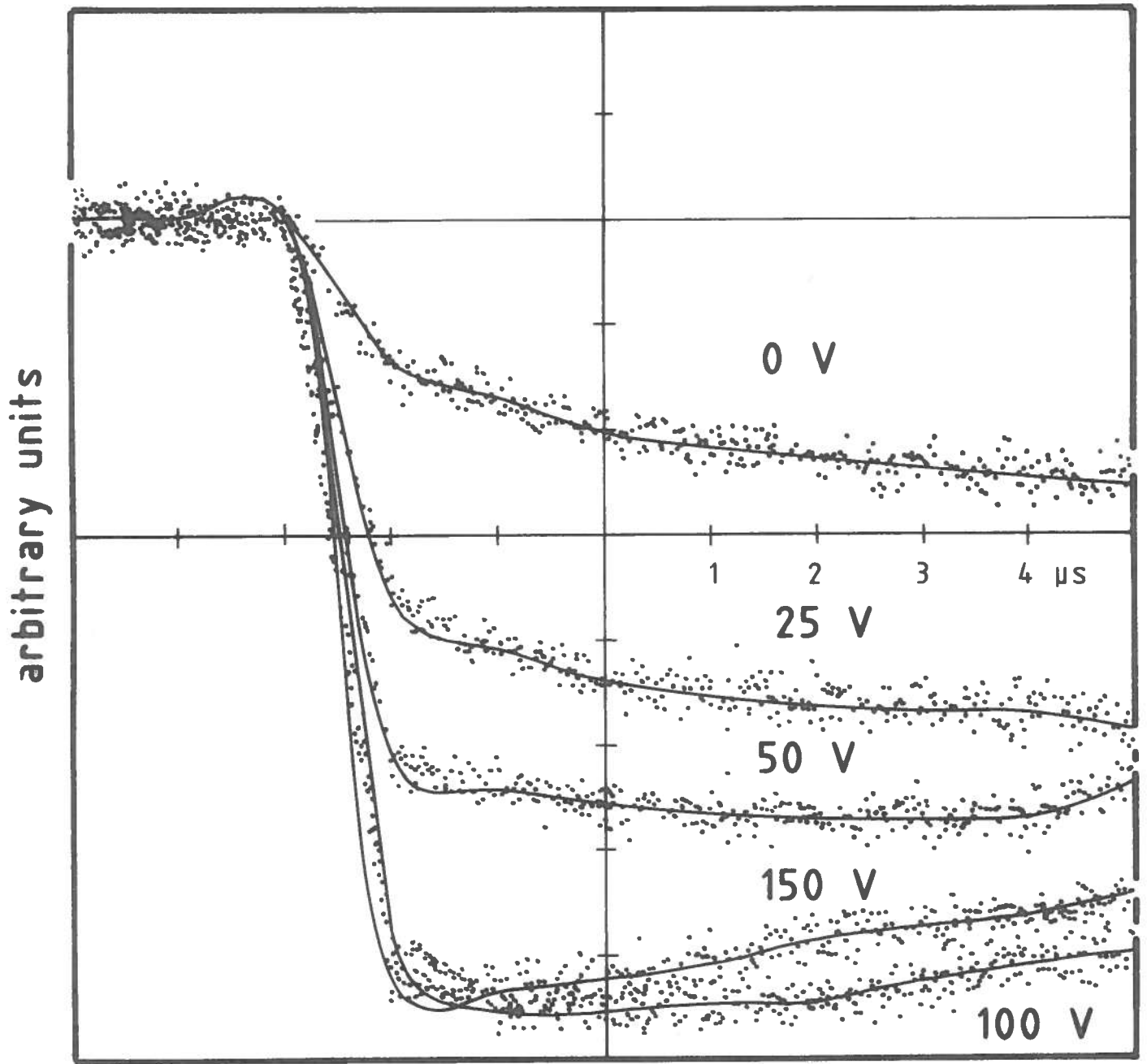


FIG.2

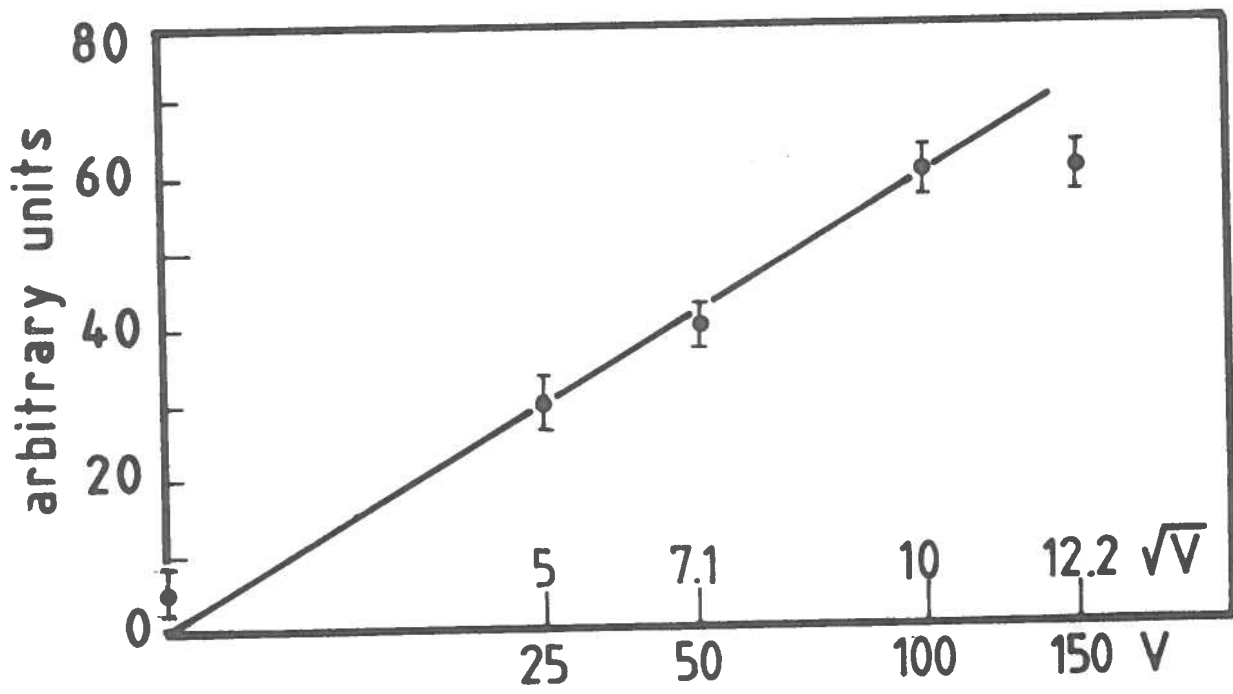


FIG.3

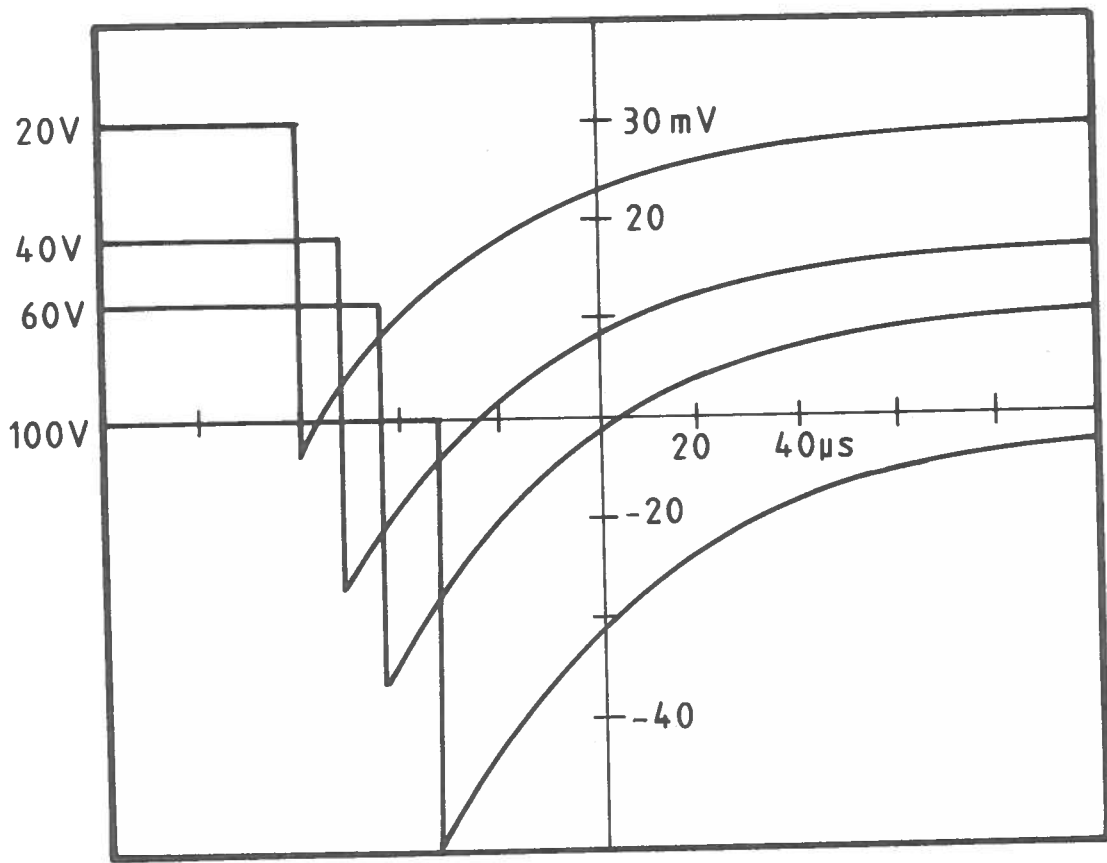


FIG.4a

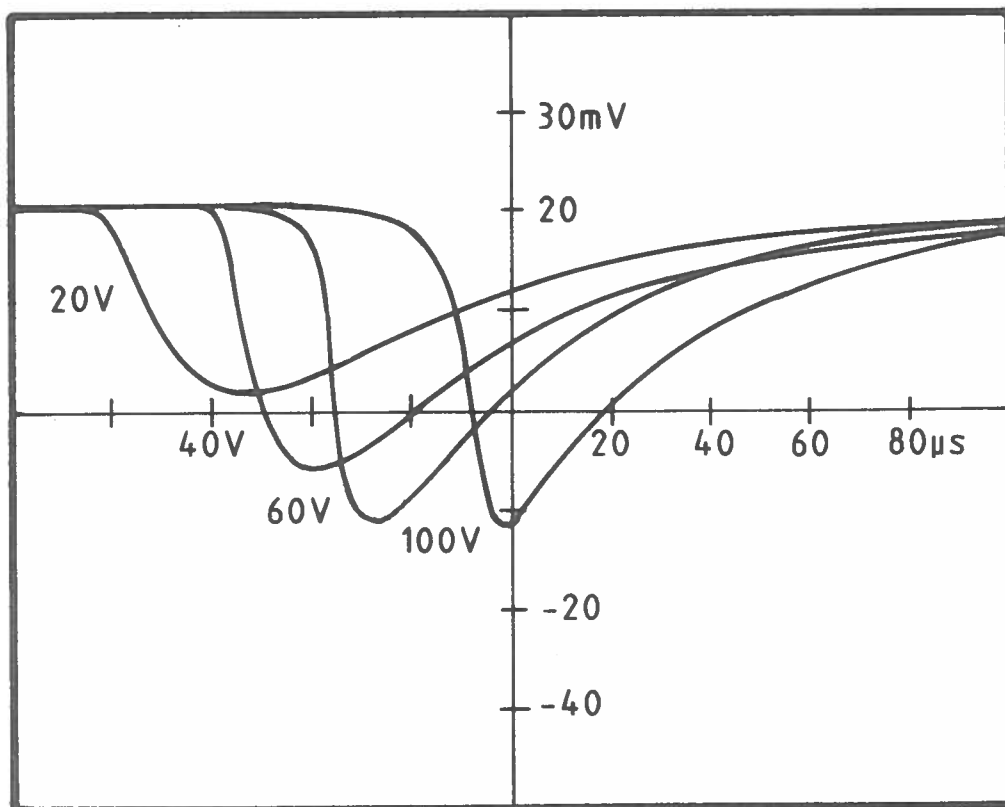


FIG.4b

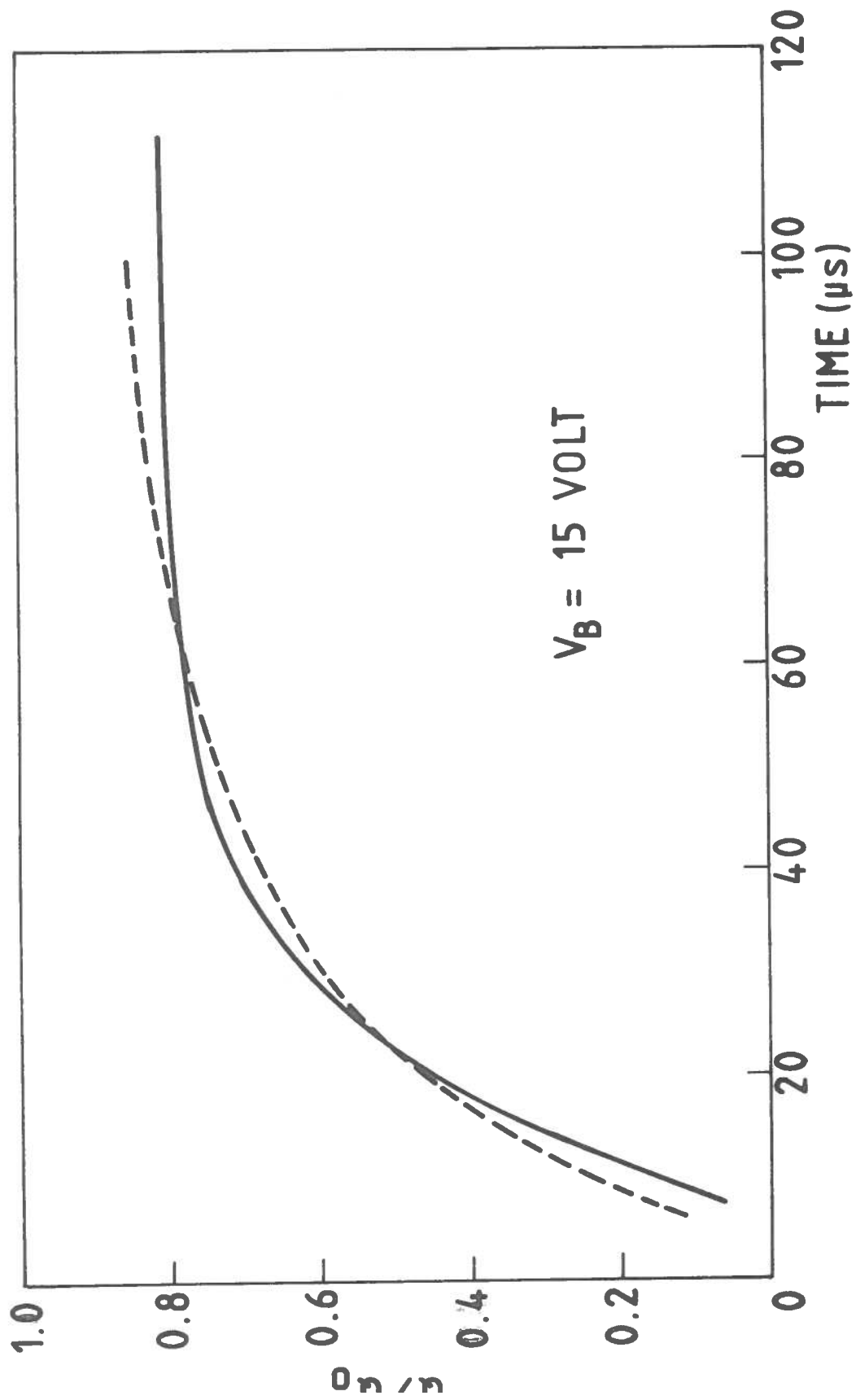


FIG.5-1

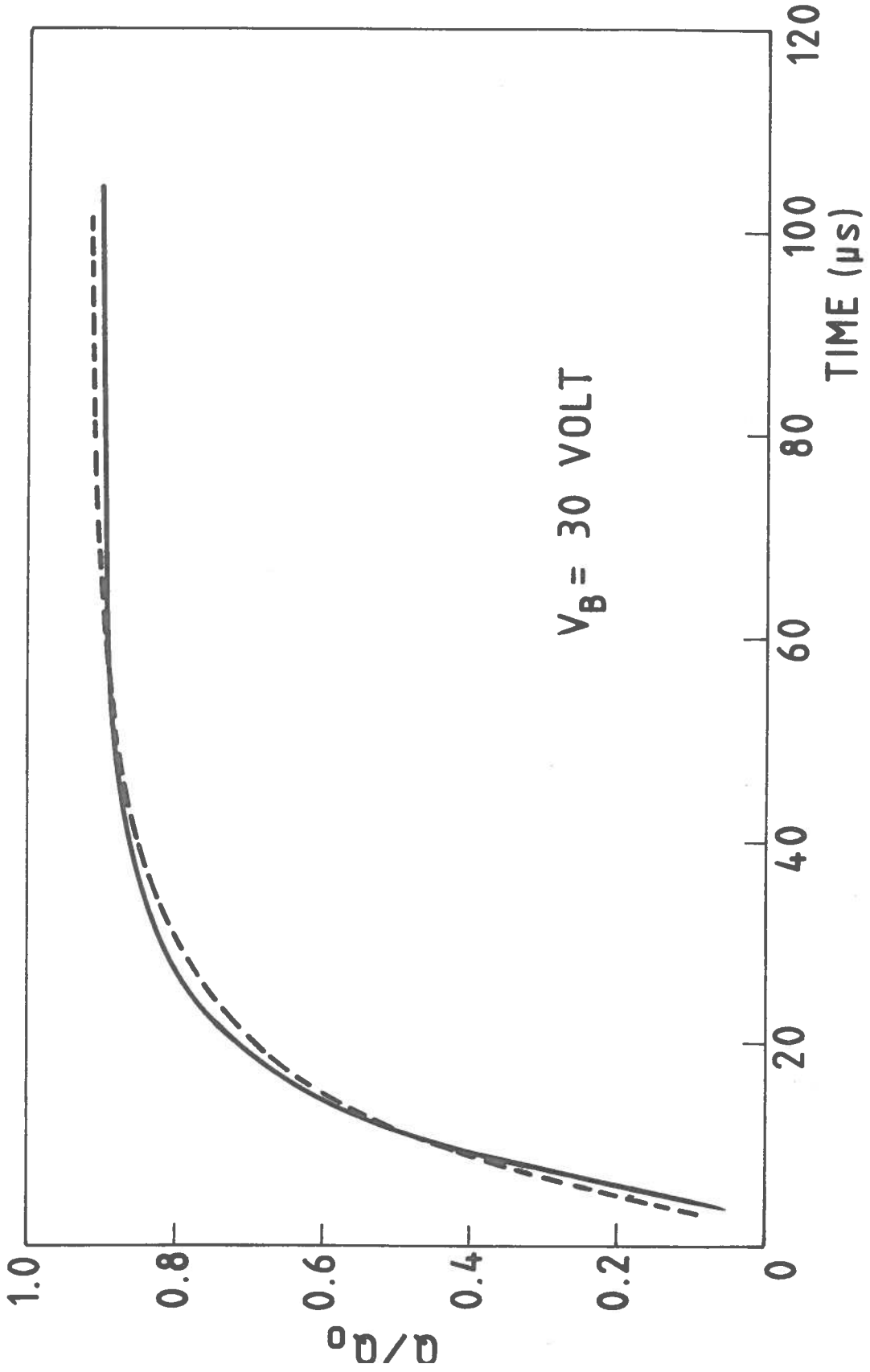


FIG. 5-2

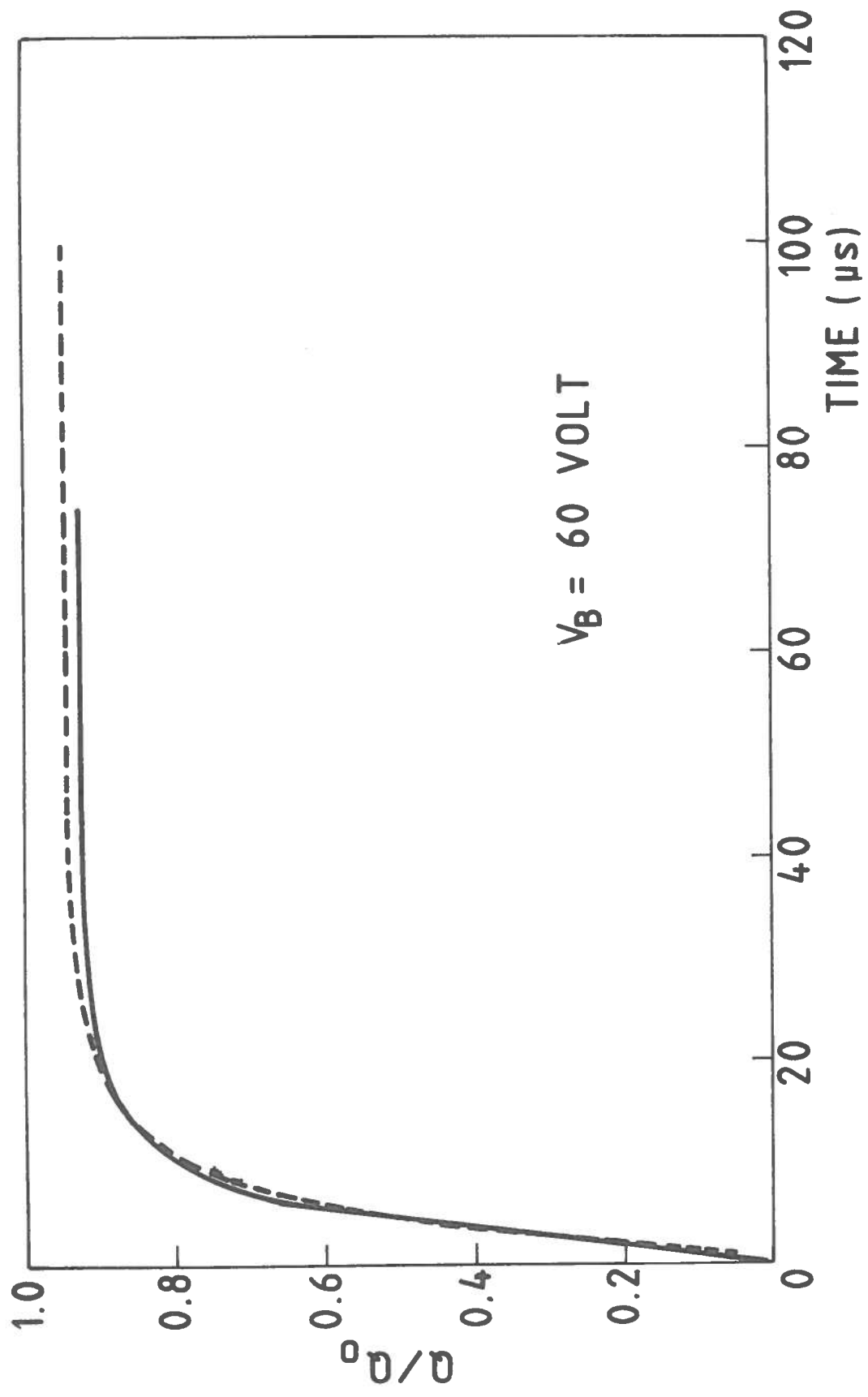


FIG. 5-3



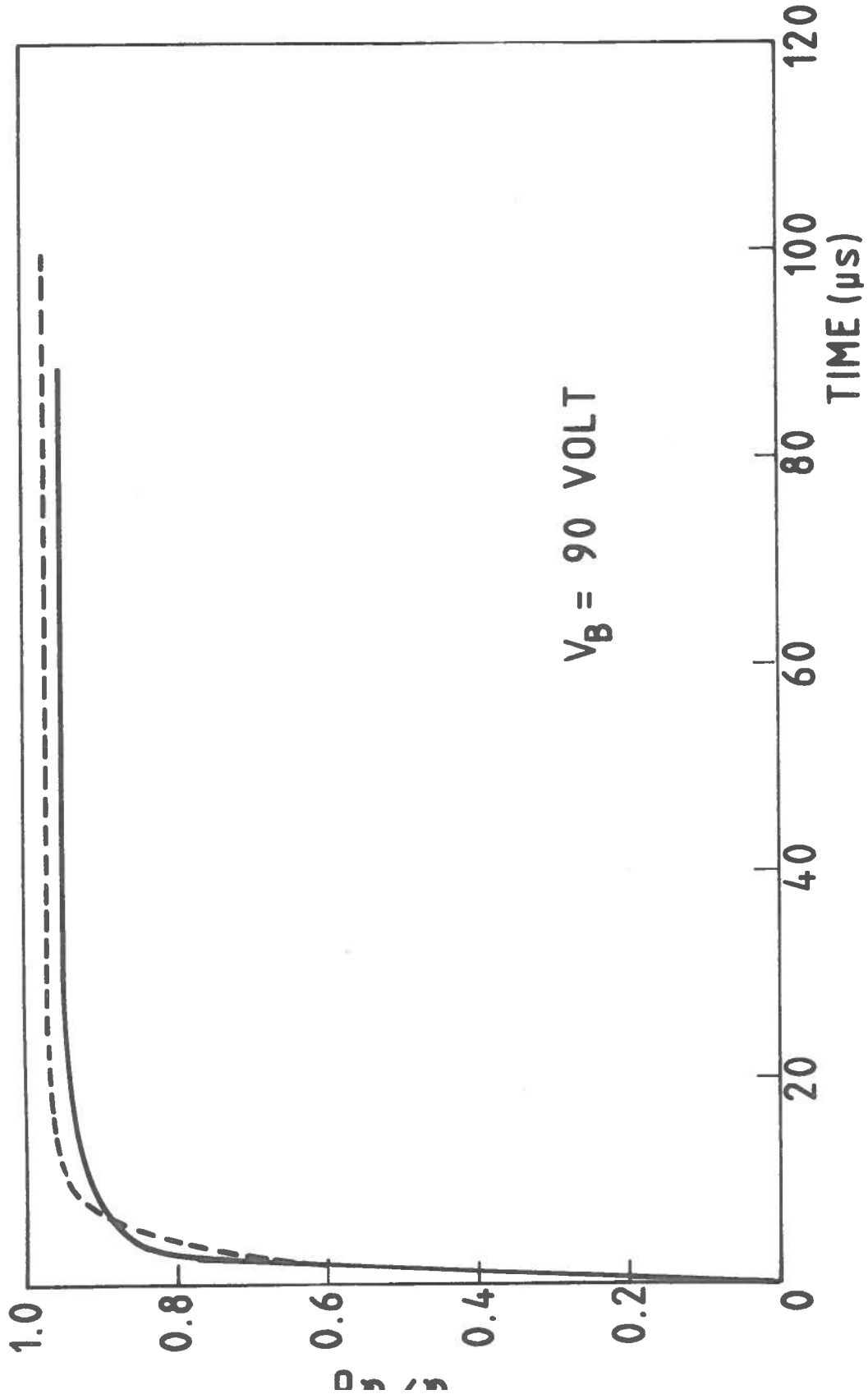


FIG.5-4

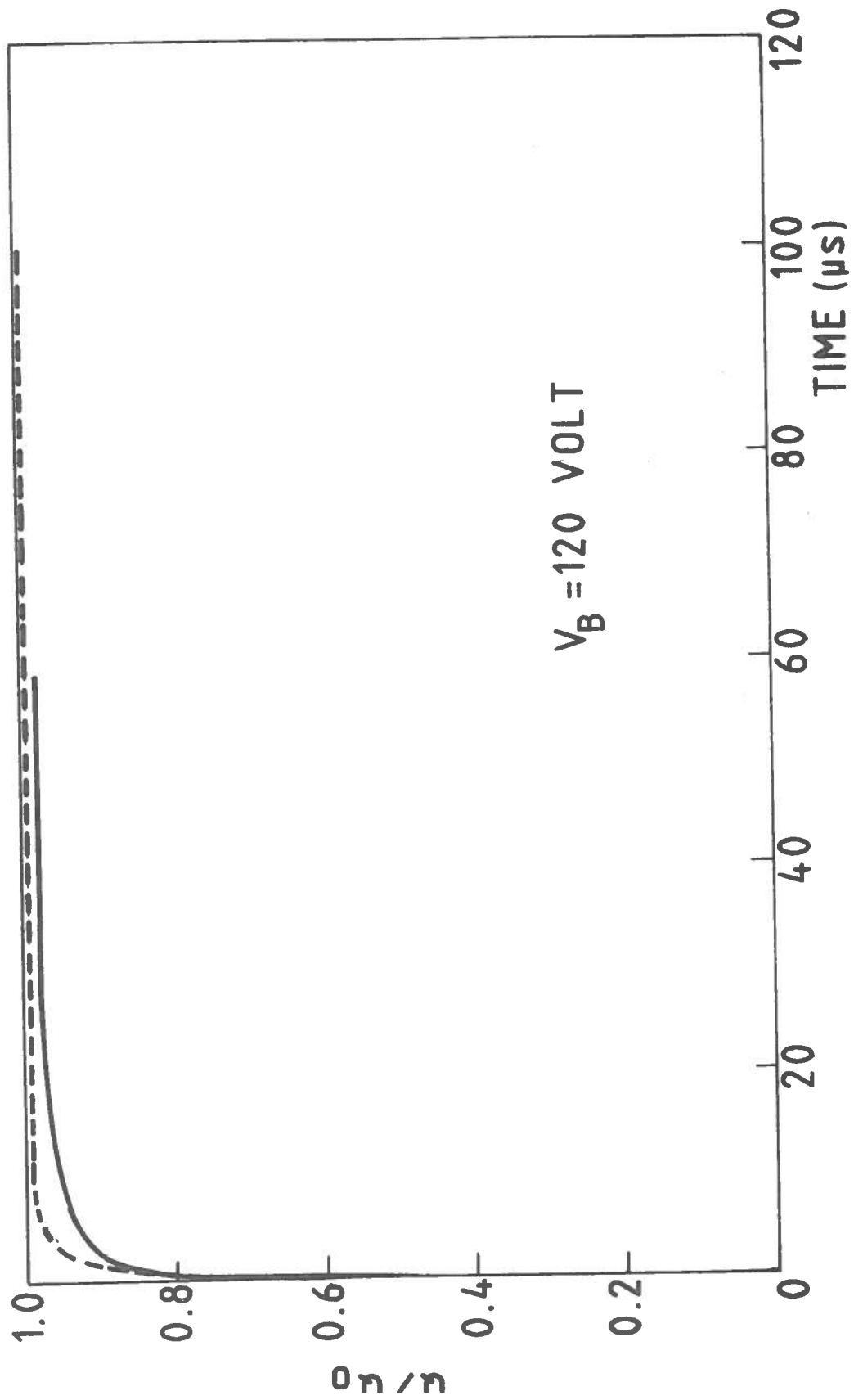


FIG.5-5

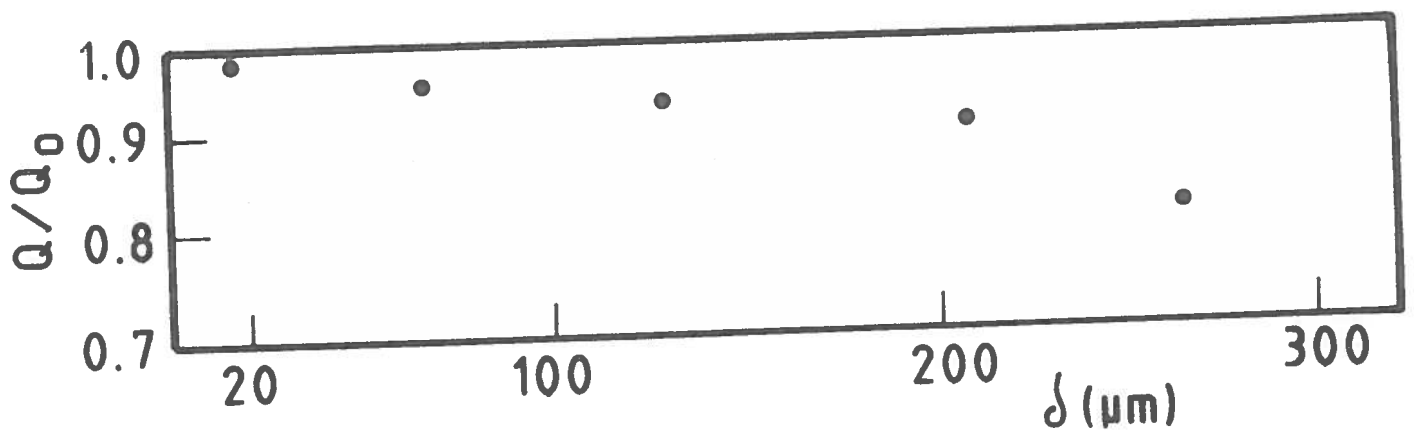


FIG.6

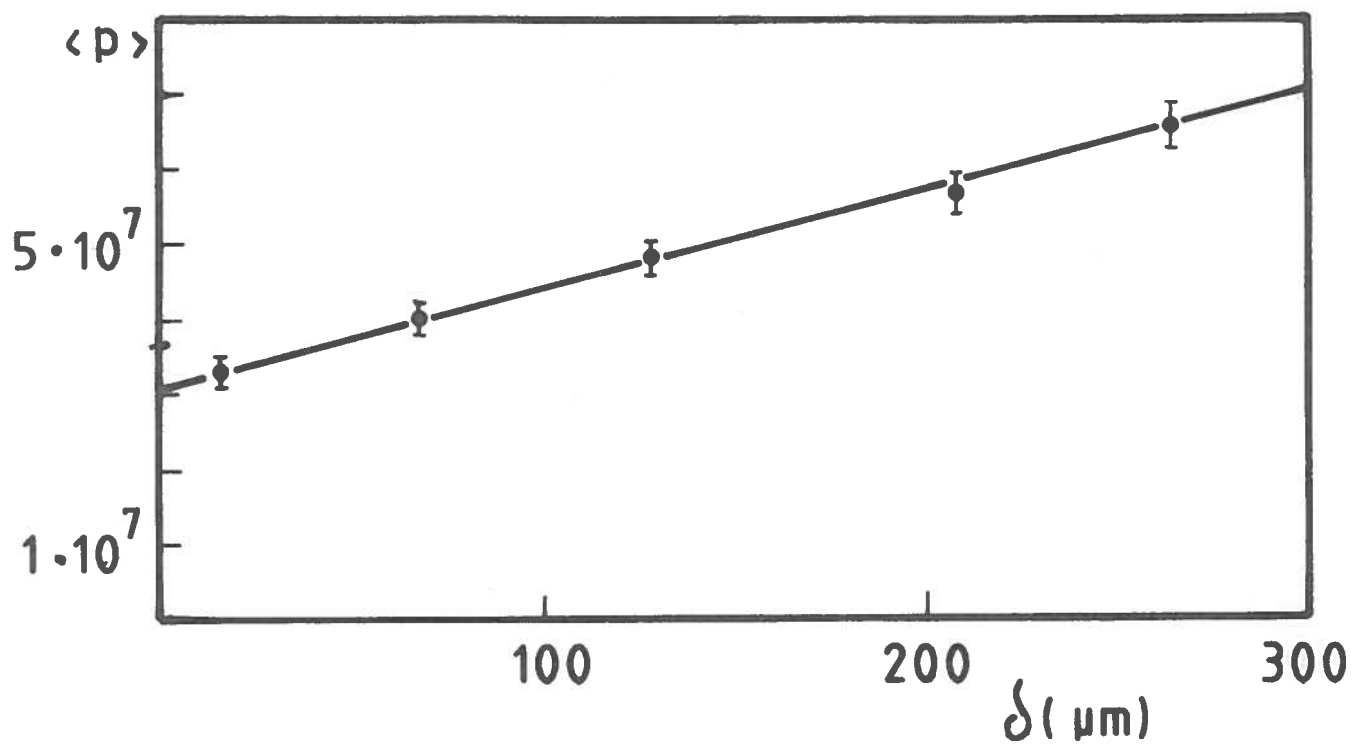


FIG.7